Volume 13, Issue 3, Page 73-81, 2024 https://doi.org/10.46810/tdfd.1487662 Research Article

BİNGÖL UNIVERSITY

Türk Doğa ve Fen Dergisi
Turkish Journal of Nature and Science
www.dergipark.gov.tr/tdfd

Testing the Reliability of Numerical Model Studies for a Broad-Crested Weir

Mahmut AYDOĞDU[1*]

[1] Malatya Turgut Özal University, Engineering and Natural Sciences Faculty, Civil Engineering Department, Malatya, Türkiye
Mahmut AYDOĞDU ORCID No: 0000-0002-7339-2442

**Corresponding author: mahmut.aydogdu@ozal.edu.tr*

(Received: 21.05.2024, Accepted: 19.08.2024, Online Publication: 26.09.2024)

Keywords
Weir,
Flow rate,
Broad-crested weir,
Ansys-fluent,
Free water surface profile

Abstract: The increase in population causes the need for water to increase day by day. The fact that water resources are limited further emphasizes the effective use of water. For this purpose, level-flow control of water transmitted through open channels is very important. Broad-crested weir types are widely used in these controls carried out through weirs. This study used a newly designed broad-crested weir type that had not been used before. The model created in the laboratory environment was tested for Q=7.84 l/s and Q=14.86 l/s flow rates. The experiments measured water surface profile, flow depths, and velocity values. The same model was tested in the numerical environment under similar flow conditions. For this purpose, three-dimensional solutions were performed with Ansys-Fluent software. The Realizable k-ε turbulence model, which has been tested for reliability in previous studies and is suitable for this type of broad-crested weir flows, was preferred. In the numerical solution, the VOF method was used for the water-air interface. Thus, the data belonging to the numerical model was verified using experimental data. In general, it was observed that there was an agreement between the experimental and numerical data in terms of water surface profile, flow depths and velocities. As a result of this study, it can be said that it allows different broad-crested weir designs to be tested with less cost before moving on to field applications.

Geniş Başlıklı Bir Savak İçin Sayısal Model Çalışmaların Güvenilirliğinin Test Edilmesi

Anahtar Kelimeler
Savak,
Debi,
Geniş-başlıklı savak,
Ansys-fluent,
Serbest su yüzü profili

Öz: Nüfusun artması suya olan ihtiyacın da her geçen gün artmasına neden olmaktadır. Su kaynaklarının kısıtlı olması ise, suyun etkin kullanımını daha da ön plana çıkarmaktadır. Bu amaçla açık kanallar vasıtasıyla iletilen suların seviye-debi kontrolü çok önemlidir. Savaklar aracılığıyla yapılan bu kontrollerde geniş başlıklı savak tipleri yaygın olarak kullanılmaktadır. Bu çalışma kapsamında daha önce kullanılmamış yeni tasarlanmış geniş başlıklı bir savak tipi kullanılmıştır. Laboratuvar ortamında oluşturulan model, Q=7.84 l/s ve Q=14.86 l/s debi değerleri için test edildi. Yapılan deneylerde su yüzü profili, akım derinlikleri ve hız değerleri ölçüldü. Aynı model benzer akım koşullarında sayısal ortamda da teste tabi tutuldu. Bu amaçla Ansys-Fluent yazılımı ile üç boyutlu çözümler gerçekleştirildi. Daha önce yapılmış çalışmalarda güvenilirliği test edilmiş ve bu tip geniş başlıklı savak akımlarına uygun olan Realizable k-ε türbülans modeli tercih edilmiştir. Sayısal çözümde su-hava arakesiti için VOF metodu kullanılmıştır. Böylece sayısal modele ait veriler, deneysel veriler kullanılarak doğrulandı. Genel olarak deneysel ve sayısal veriler arasında; su yüzü profili, akım derinlikleri ve hızları bakımından uyum olduğu görülmüştür. Bu çalışma neticesinde saha uygulamalarına geçmeden önce, yapılacak farklı geniş başlıklı savak tasarımlarının daha az maliyetle test edilmesine imkân sağladığı söylenebilir.

1. INTRODUCTION

For the effective and sustainable use of limited water resources, it is necessary to determine the distribution of water over time and space in terms of properties and volume. In Türkiye, water consumption is mostly used for agricultural purposes and is transmitted through open channels. In this type of transmission, the amount of

water in the channel must be measured regularly and reliable records must be kept. Because this is essential to protect existing water and increase usage efficiency. In general, flow measurements are made with a method that is costly and requires intense effort, such as velocity-area measurements [1]. However, low-cost, reliable, and practical methods are needed for flow measurement in open-channel flows. One of these methods is measurement weirs. Weirs are widely used in irrigation channels and environmental projects. Built-in streams and open channels increase the irrigation capacity by raising the water level upstream, storing water, or directing the flow by weirs [2]. Weirs are constructed in various geometric types (labyrinth, ogee, broad-crested, and sharp-edged) depending on the need. The broad-crested weir type is widely used in field practices [3]. Compared to other types, broad-crested weirs have many advantages, such as structural stability, low cost, and extremely low sensitivity to tailwater submergence [4]. In literature, the hydraulic properties of broad-crested weirs with different geometries and designs were examined and many experiments were conducted for this purpose [4]–[7]. These studies focused on determining the flow coefficient and revealing the effect of geometries on the flow pattern.

Many studies have been carried out previously on the broad-crested weir structure. Clemmens et al. [8] examined the flow change and energy loss in upstream and downstream conditions using a rectangular broad-crested weir. They reported that upstream face slopes of 3:1 and 2:1 were acceptable to accurately predict flow. They stated that the water surface profile decreased continuously from the front face slope to the end of the narrowing part of the weir, and did not affect the flow estimation of the downstream water level. Flow over a trapezoidal broad-crested weir at different upstream and downstream slopes was investigated by Sargison, J. E., & Percy, A. [9]. In general, pressure and water surface profiles were similar for all test cases. Vertically increasing the upstream slope reduced the height of the water surface profile and the static pressure affected the weir. They also stated that it also reduced the flow coefficient. Azimi et al. [10] examined the flows passing over the broad-crested weir sloped upstream and downstream directions. They also collected experimental results available in the literature and suggested useful correlations for the flow coefficient. Madadi et al. [11] investigated the effect of the upstream front slope of rectangular broad-crested weirs on wavy weir flow. The results obtained showed that when the weir upstream slope decreased from the standard angle, that was, from 90° to 40°, the relative wave height decreased by up to 78% and the relative wavelength increased by up to 55%.

However, in some cases, experimental studies cause an economic burden and serious time loss. The solution is to use today's technology effectively and efficiently. Nowadays, physical modeling can be done quickly and practically in a digital environment with advanced computer and software technologies. In particular, computational fluid dynamics (CFD) simulations are advantageous over physical modeling by easily solving many different parameters and flow situations [12]. In addition, numerical model results are verified with physical models, providing the opportunity to analyze different flow environments and water structures. There are recent studies in the literature for this purpose. Sarker and Rhodes [13] investigated the open channel flow over a rectangular broad-crested weir experimentally and theoretically. The basic equations governing the flow were solved numerically using the CFD-based Fluent program. The findings obtained from the studies were compared and found to be consistent with each other. Bal [14] measured the velocity field of the flow passing over a broad-crested weir under two different flow conditions using one-dimensional Laser Doppler Anemometer. He used the Ansys-Fluent package program based on the finite volume method for numerical solutions. As a result of the comparison of numerical and experimental data, it was stated that the RNG k-ε turbulence model gave more successful results. Felder et al. [15] carried out an experimental study to determine the water surface profile, velocity, and pressure distributions on a broad-crested weir flow. They analyzed the flow characteristics on the crest by considering non-uniform velocity distributions and non-hydrostatic pressure distributions. They stated that the data differed from the smooth turbulent boundary layer theory but were consistent with previous studies on this subject. Soydan et al. [16] tested and compared the trapezoidal cross-section broad-crested weir structure with experimental data with the help of an Ansys-Fluent numerical solver. In the numerical solution,Standard k-ε, Renormalization group k-ε, and Realizable k-ε turbulence models were used. Water surface profiles were determined with VOF. The flow profiles were compared with numerical and experimental data and it was stated that the turbulence models used were quite successful in predicting the flow profiles.

İlkentapar & Öner [17] examined the water surface profiles and velocity distributions upstream and downstream of the rectangular broad-crested weir by using three different flow rate values. Again, they created numerical models under the same flow conditions as the experiments and realized solutions with the FLOW-3D package program. Using different mesh structures and Standard k-ε turbulence models, water surface profiles were determined by the volume of fluid method. The water surface profiles and velocity distributions obtained from the solution were compared with experimental data. Yıldız & Yarar [18] experimentally examined the effects of broad-crested weir models with different slope angles on the flow. 41 different flow rates were tested for three different broad-crested weir models. They also performed numerical solutions under the same flow conditions with Ansys-Fluent, a CFD software. It has been concluded that the experimental and numerical model results are compatible.

This study used a newly designed broad-crested weir type that had not been used before. Such a design aims with different surface slopes weir, to experimentally

measure the water flow movement in the channel and investigate its numerical reliability. For this purpose, the upstream surface of the broad-crested weir was designed as trapezoidal and the downstream surface as circular in the model created in the laboratory environment. The experiments were carried out for Q=7.84 l/s and Q=14.86 l/s flow rates. In the experiments, the water surface profile, flow depths, and velocity values were measured. Then, the same model was tested in the numerical environment under similar flow conditions. In the numerical study, three-dimensional numerical simulations were carried out with the Ansys-Fluent software, which provides solutions with the finite volume method. The reliability of the previous studies was tested and the Realizable k-ε turbulence model, which is suitable for this type of broad-crested weir flows, was preferred. The water surface profile was calculated with the Volume Of Fluid (VOF) method and the solutions were carried out in three dimensions. The water surface profiles, flow depth, and velocity values of the numerical solution were compared with the experimental measurement results.

2. MATERIAL AND METHOD

The flow over a broad-crested weir under commonly used free-flow conditions is shown in Figure 1 below [19].

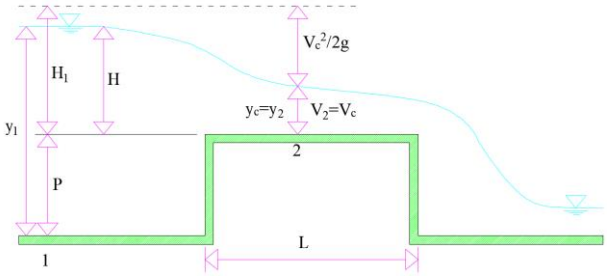

Figure 1. Flow conditions over a broad-crested weir

In Figure 1, H is the water height above the weir surface at the upstream, H_1 is the total energy height at the upstream, y_1 is the water depth at the upstream, y_c is the critical depth, V_c is the critical velocity and P is the weir height. The total energy height H_1 at the upstream is calculated as in Equation 1.

$$H_1 = y_c + \frac{V_c^2}{2g} = \left(\frac{3}{2}\right) y_c \qquad (1)$$

The critical velocity is calculated as in Equation 2.

$$V_c = \sqrt{g y_c} \qquad (2)$$

In literature, broad-crested weirs are classified according to H/L value. Accordingly, if 0.1≤H/L≤0.35, the critical flow control is upstream of the weir, and the flow coefficient changes slowly in this range and is called a broad-crested weir [19].

In this study, experimental measurements were carried out by taking two different flow rates into account to determine the flow velocity and water surface profiles passing over the broad-crested weir with different upstream and downstream surfaces. The experiments were carried out with the help of a rectangular cross-section open channel model in the Civil Engineering Hydraulics Laboratory of İnönü University (Figure 2).

Figure 2. Open channel model used in the experimental

The bearing elements of the experimental setup were made of steel. The channel side walls were made of transparent plexiglass material for easy observation of the flow. There are two reservoirs at the beginning and end of the channel, which circulated the water in the channel. This open channel model had a length of 12.8 m, a width of 0.40 m, and a height of 0.5 m. A digital limnimeter with a sensitivity of 0.1 mm in the depth of the flow was used, and a pump with a capacity of 0-360 m^3/hour with an inlet and outlet diameter of 8 inches was used to circulate the water in the channel arrangement. To measure the flow rate, a TMF2011-C model electromagnetic flowmeter with ± 0.5% accuracy was used between the pump and the inlet valve. In addition, the flow control was monitored precisely and instantly using the Programmable Logic Controller (PLC) control method, which works with a remote sensing system. PLC software can be controlled via smartphone and second-by-second flow rate readings can be easily viewed. Figure 3 showed the PLC control system working mechanism.

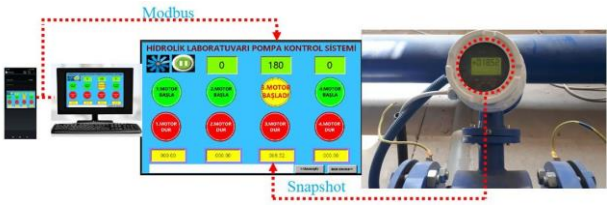

Figure 3. PLC control system working mechanism

The broad-crested weir was placed 6.5 m downstream from the point where the water inlet the channel. Since this 6.5 m point was the starting point of the weir, it was taken into account as the 0 (zero) point in the measurements. The total weir length was 1 m, and flow depth measurements were taken at 0.1 m intervals towards the downstream way, starting from the zero point upstream at -0.6 m. Flow depths over the weir were measured at 0.05 m intervals. Schiltknecht MiniAir20 model velocity meter with ±0.5% accuracy was used to measure the flow velocity. It can detect velocity values up to a maximum of 5 m/s with a measurement velocity of 2 measurements/second. The average button for all velocity values was activated and at least 240 seconds were waited for each measurement. The velocity meter was placed on a scale with a wheeled mechanism that

can move forward-backward and left-right on the flow channel. To minimize experimental setup errors, the devices and equipment used in experiments were provided by İnönü University administration at regular intervals (once every 6 months). However, in model studies, some inevitable errors caused by scale effects are also known to affect the results. On the other hand, the fact that the equations that manage the movement of the water contain viscosity and turbulence expressions makes it difficult to solve such problems. Nowadays, the widespread use of CFD methods for solutions of water structures-flow interaction problems has enabled significant developments in calculations and economic, fast, and easy solutions in the analysis of open-channel flows.

2.1. Numerical Model Setup and Basic Equations

Within this study, the physical model, whose experiments were carried out in a laboratory environment, was also created in a numerical environment through Ansys-Fluent software. For this purpose, free surface flow over a broad-crested weir was examined. To examine the mean flow characteristics of broad-crested flows, the Navier-Stokes equations were used. The main equations used in the numerical model and defining the flow are presented below [20]:

$$\frac{\partial \rho}{\partial t} + \nabla.(\rho \boldsymbol{U}) = 0 \tag{3}$$

$$\frac{\partial(\rho \boldsymbol{U})}{\partial t} + \nabla.(\rho \boldsymbol{U} \otimes \boldsymbol{U}) = -\nabla p + \nabla.\boldsymbol{\tau} + S_M \tag{4}$$

$$\boldsymbol{\tau} = \mu\left(\nabla \boldsymbol{U} + (\nabla \boldsymbol{U})^T - \frac{2}{3}\boldsymbol{\delta}(\nabla.\boldsymbol{U})\right) \tag{5}$$

Here, ρ is defined as density, ∇ as gradient operator, $\boldsymbol{U}$ as velocity vector, t as time, $\boldsymbol{\tau}$ as stress tensor, S_M as source term, μ as viscosity, $\boldsymbol{\delta}$ as identity matrix. Equation 3 refers to the continuity equation, and Equation 4 refers to the conservation of momentum [21].

In this study, the two-equation Realizable k-ε model was preferred. Two-equation turbulence models allow the determination of a turbulent length and time scale by solving two separate convection equations. The Realizable k-ε model is a model based on model transport equations for turbulent kinetic energy (k) and its dissipation rate (ε). The Realizable k-ε model differs from the Standard k-ε model with two important features. The Realizable k-ε model includes an alternative turbulent viscosity formula. A modified convection equation for the dissipation ratio ε is derived from an exact equation for the transport of mean-square vorticity fluctuation. In the Realizable k-ε model, the transport equations for k and ε values are as follows.

$$\frac{\partial}{\partial t}(\rho k) + \frac{\partial}{\partial x_j}(\rho k u_j) = \frac{\partial}{\partial x_j}\left[\left(\mu + \frac{\mu_t}{\sigma_k}\right)\frac{\partial k}{\partial x_j}\right] + G_k + G_b - \rho\varepsilon - Y_M + S_k \tag{6}$$

$$\frac{\partial}{\partial t}(\rho \varepsilon) + \frac{\partial}{\partial x_j}(\rho \varepsilon u_j) = \frac{\partial}{\partial x_j}\left[\left(\mu + \frac{\mu_t}{\sigma_\varepsilon}\right)\frac{\partial \varepsilon}{\partial x_j}\right] + \rho C_1 S\varepsilon - \rho C_2 \frac{\varepsilon^2}{k+\sqrt{v\varepsilon}} + C_{1\varepsilon}\frac{\varepsilon}{k}C_{3\varepsilon}G_b + S_\varepsilon \tag{7}$$

Here; G_k denotes the formation of turbulent kinetic energy depending on the gradient of the average velocity, G_b denotes the formation of turbulent kinetic energy due to buoyancy, Y_M denotes the contribution of undulating expansion in compressible turbulence to the total dissipation rate. C_2 and $C_{1\varepsilon}$ are constants. σ_k and σ_ε are the turbulent Prandtl numbers for k and ε respectively, and S_k and S_ε are user-defined source terms. Except for the constants in the model, the k equation here is the same as the k-ε model and the RNG k-ε model. However, the ε equation is quite different from standard and RNG-based equations. The validity of this model has been widely recognized for a wide variety of flows, including rotating homogeneous shear flows, free flows containing jets and mixing layers, and channel and boundary layer flows. Compared to the Standard k-ε model, the Realizable k-ε model yields better predictions for certain flows. One example is the round jet, for which the Standard k-ε model overestimates the spreading rate. Generally, since the realizability conditions are approached asymptotically, the turbulence characteristics are more consistent than for the Standard k-ε model. The Realizable k-ε model uses wall functions and has the same default initial conditions and scalings as the Standard k-ε model [21].

2.2. Solution Region Boundary Conditions with Volume of Fluid Method

In open channel flows, the interface between two-phase immiscible fluids (such as water and air) can be examined using the volume of fluid method, which can be applied to a constant Eulerian relation [22]. This method determines the parts of the solution region that are filled with water and air. The working principle of the numerical modeling system is defined by the fluid volume, which indicates the volumetric occupancy rate in the created solution region. The method called VOF is used as a powerful and successful technique in determining the free surface shape in open channel flows. This method is based on a process that determines the filling rates of the element volumes of the fluid entering a given numerical calculation network at certain time intervals and accordingly calculates the free surface profile in the flow at selected time intervals. The VOF method tracks the moving front by adopting an implicit formulation using the volume fraction of one phase in each cell of a discretized domain. This method has the advantage of conserving the total volume by construction. However, its main disadvantage is that it increases the model complexity and should be preferred only when there are multiphase problems. If the element in the calculation network within the solution region is fully filled, it takes the value F=1, and when it is empty, that is, filled with air, it takes the value F=0. For 0>F>1, the network element is partially filled. VOF was also preferred for this study examining the broad-crested weir structure.

In this study, the model geometry was created with Solidworks software and transferred to Ansys-Fluent software with (.step) extension. Since channel length and mesh number directly affect the solution time, especially in numerical solutions, the channel geometry was kept a little shorter so as not to change the flow conditions. For the numerical solution; flow rate values, flow velocities, and weir size values were taken as the same as the experimental values at the channel inlet. Here, y_1 is the water depth upstream, and V_1 is the inlet velocity water in the channel, Y is channel height, b is channel wide, and Z total channel length. The Y value was taken as 0.3 m for the numerical solution, while the experimental model channel size was 0.5 m. The Z value in the experimental model was 12.8 m, it was taken as 7 m in the numerical model. For the numerical solution, the weir was placed 2 m from the upstream. Table 1 includes experimental and numerical data.

Table 1. Summary of experimental and numerical data

Q (l/s)	y_1 (m)	V_1 (m/s)	Numerical Channel Dimensions (b*Y*Z) (m)	Experimental Channel Dimensions (b*Y*Z) (m)
7.84	0.1775	0.11	0.4*0.3*7	0.4*0.5*12.8
14.86	0.2064	0.18	0.4*0.3*7	0.4*0.5*12.8

Also, the dimensions of the broad-crested weir used in the numerical solution were given schematically in Figure 4. FD represents the direction of the flow.

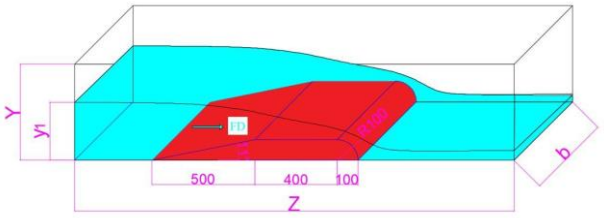

Figure 4. Schematic drawing of the broad-crested weir (Figure numerical dimensions are in mm)

The mesh designate was first made appropriate with the numerical solution's channel structure. Linear mesh structure was preferred because the channel geometry and weir structure did not have too many curvilinear and variable surfaces. The optimum number of meshes was achieved by running the model several times with different numbers of meshes and convergence of the solution network. In this study, instead of considering the effect of different mesh types on modeling, linear mesh structure was preferred. Because the model geometry was not too complex and there were not very small areas on the weir. For solution sensitivity, Orthogonal Quality and Skewness values were taken into account and solutions were performed for Coarse, Medium, and Fine mesh structures. As a result, the Fine mesh structure, which obtained the closest result to the experimental data, was considered. As a result of the solutions, the Average Orthogonal Quality value was obtained as 0.99863 and 0.99864. Again, the Average Skewness value was obtained as 0.00948 and 0.0092. These values indicate that the mesh quality was within the accepted limits [21]. Figure 5 shows an image where the mesh structure and boundary conditions were defined. In Figure 5, B inlet was defined to the system as "velocity inlet" and the experimentally measured flow velocity value was taken into account. F channel outlet is defined as “pressure outlet”. In addition, the part of the D channel outside the flow area is defined as a "pressure outlet" since it is a surface opening to the atmosphere. A and E represent the right and left side surfaces of the channel, respectively, and are defined as "wall". C is the bottom of the channel and is defined in the system as a "wall".

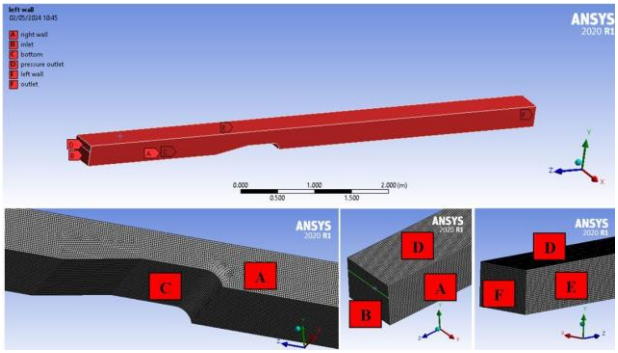

Figure 5. Boundary conditions defined for the numerical model

After data entry was provided at all these stages with Ansys-Fluent software, the analysis was started by taking Δt = 0.02 seconds and Number of time steps = 3500. The iteration convergence value for all solutions was taken into account as 0.000001 ($1x10^{-6}$) in all equation values to stay on the safe side. As a result of the analysis, water surface profiles, flow depths, and velocity values were obtained numerically, taking into account the experimental measurement points in the channel. Thus, the reliability of the study was tested by comparing the experimental and numerical solution results.

3. RESULTS AND DISCUSSION

This study measured the velocities of the flow passing over the broad-crested weir, whose upstream surface was trapezoidal and its downstream surface was circular, and the depths at certain points over the weir and along the experimental set were measured. Thus, water surface profiles were obtained. Solutions were taken for two different flow rates in experimental and numerical measurements, considering the same flow conditions. Numerical simulations were carried out with Ansys-Fluent software, which works with the finite volume method. Using the Realizable k-ε turbulence model, the water surface profile was calculated with the VOF method, and the solutions were obtained in three dimensions. Then, the water surface profiles of the numerical solution were compared with the experimental measurement results. Figure 6 shows the water surface profiles obtained experimentally and numerically along the (z) channel direction for Q=7.84 l/s and Q=14.86 l/s. The values were measured at 10 cm intervals, starting 60 cm before the weir in the upstream direction, in both the experimental and numerical models. The part where the weir begins was accepted as the zero (0) starting point, and flow depths were measured at 5 cm intervals on the

weir. After the weir, flow depths were again measured at 10 cm intervals, and at the points where the depth change decreased, measurements continued at 20 cm intervals until the end of the channel. The flow depths measured (h) in the figure were made dimensionless by dividing by the maximum flow depth (h_{max}), and a water surface profile was created along the direction (z) in the channel. It had been observed that the flow depths were generally compatible with two flow rates each other. It was seen that more sensitive results were obtained in numerical solutions, especially in the circular surface transition from upstream to downstream. In this section, separations in the streamlines can be seen due to the increase in flow velocity. It can also be said that experimentally and numerically closer flow depths were obtained towards the downstream of the channel. When we compare the flow depths for Q=7.84 l/s and Q=14.86 l/s flow rates, a slight difference was revealed. For Q=7.84 l/s flow rate, the experimentally measured flow depths after the broad-crested weir were higher than the numerical study, while for Q=14.86 l/s flow rate, the numerical results were lower. This situation showed that the numerical studies achieve more sensitive results with the appropriate mesh structure. In addition, since the external human intervention of the flow field was less and the roughness conditions of the weir and inside the channel were clearer, such a difference was acceptable. Once more, the differences between the numerical and experimental solutions may be affected by the mesh structure of the flow in the channel, the mesh type, the selected solution model, the vortex, and turbulence movements of the flow in the channel due to the weir structure. Therefore, the values may change in cases where the flow accelerates or passes downstream from the weir surface. As can be seen from the flow topology, for flow rates Q=7.84 l/s and Q=14.86 l/s, there was no separation of boundary layers upstream and at the top of the broad-crested weir. This reflects the difference between our designed weir and one of the other broad-crested weirs with different cross sections [14].

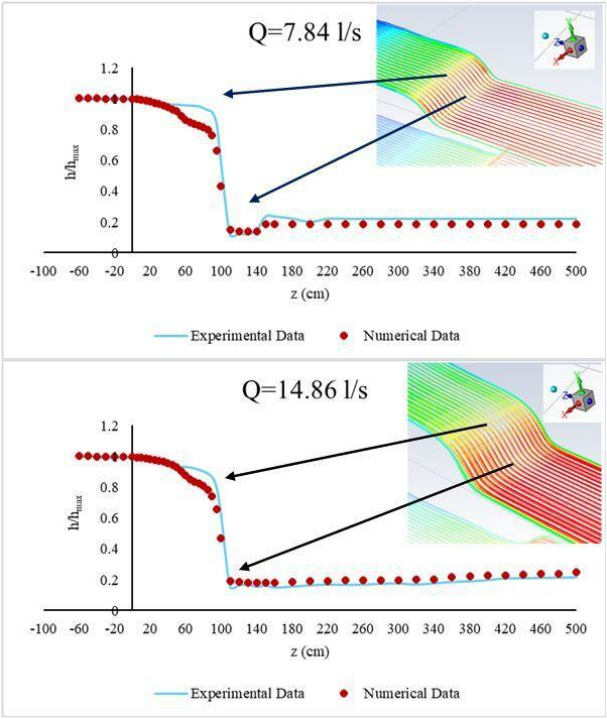

Figure 6. Experimental and numerical water surface profile for Q=7.84 l/s and Q=14.86 l/s

Figure 7 showed that the static pressure values affected over the channel bottom. In general, a high-pressure value that would cause deformation at the channel bottom was not observed. Maximum static pressure values were observed on the upstream aspect for Q=7.84 l/s and Q=14.86 l/s. When the two flow rates were compared, higher static pressure values were obtained for the flow rate Q=14.86 l/s. Both of two flow rates it was observed that the pressure decreased to negative values only at the weir exit, on the curved surface where the flow started to accelerate. For the broad-crested weir surface, only the curved surface can be coated with a more durable coating material against the risk of cavitation. Thus, possible damage to the weir surface was prevented.

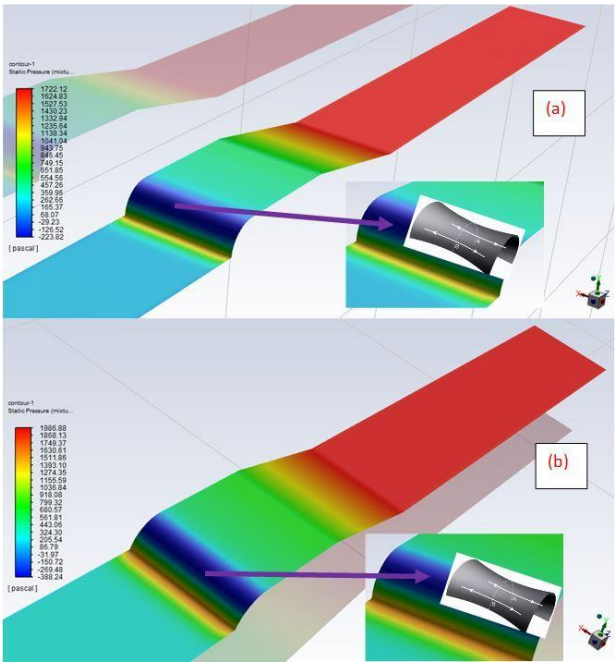

Figure 7. Static pressure values for (a) Q=7.84 l/s, (b) Q=14.86 l/s, and material example for the surface to be coated

Again, the velocity values obtained for Q=7.84 l/s and Q=14.86 l/s flow rates were given in Figure 8. The measured velocity values were the average velocity values taken at x=0.2 m for the central axis of the channel. In the numerical solution, the channel length was taken as 7 m to shorten the number of meshes and solution time. The zero (0) point in Figure 8 was the starting point of the 2 m section before the broad-crested weir upstream. In other words, the 2 m point represents where the weir begins, the beginning of the trapezoidal surface. These levels were also indicated on the velocity magnitude contours. The velocimeter average button for all experimental velocity values was activated and at least 240 seconds were waited for each measurement. Flow velocities, for Q=7.84 l/s and Q=14.86 l/s flow rates were found to be compatible numerically and experimentally. Both flow rates in upstream, flow velocity remained at very low values. Hereby, the experimental and numerically measured values were very close.

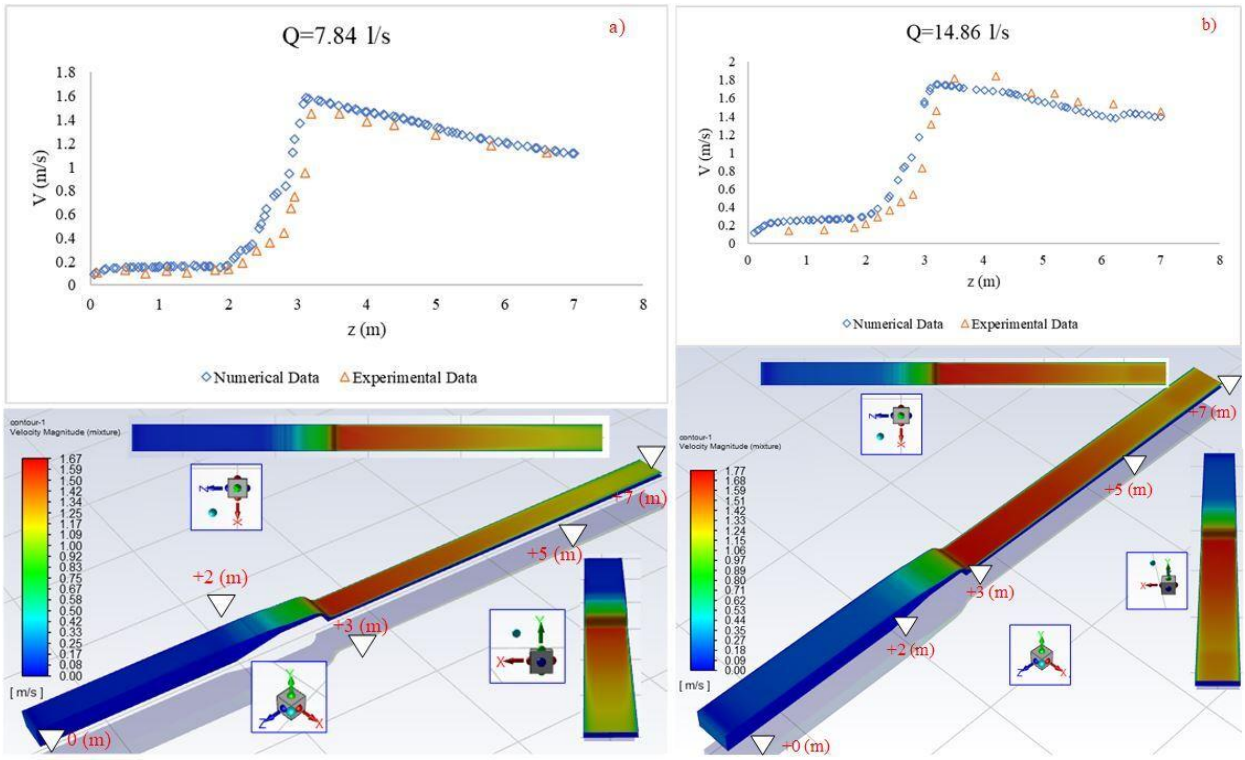

Figure 8. a) For Q=7.84 l/s experimental and numerical velocity values and velocity magnitude contours, b) For Q=14.86 l/s experimental and numerical velocity values and velocity magnitude contours

Velocity values began to increase on the weir surface and towards the points where the critical flow depth began to form, and the difference between the values obtained in the numerical and experimental solutions partially increased. When both flow rate values were compared Q=14.86 l/s flow rate value, it can be said that the experimental velocity measurements in the section after the weir are slightly higher than the numerical solution. It can be said that more precise values are obtained in the numerical solution depending on the sensitivity of the measuring device, the mesh structure of the model, and the increase in flow velocity.

4. CONCLUSION

In the context of this study, a broad-crested weir model which owns a trapezoidal upstream surface and a circular downstream surface, inhearse the channel in a laboratory environment was used. Passing over the weir flow rates, depth, and velocity, were measured. Experiments were carried out for two different flows. Then, numerical simulations were carried out to determine the flow velocity and depth over the broad-crested weir, considering the same flow conditions. Ansys-Fluent package program, which provides solutions using the

finite volume method, was used. Realizable k-ε turbulence model was used. The water-air surface interface was calculated by the VOF method. As a result of numerical solutions, three-dimensional velocity, static pressure contours, and water surface profiles were obtained.

• The water surface profiles of the numerical solution were compared with the experimental measurement results. In general, the water surface profiles were quite compatible with the experimental data. This further increased the reliability of numerical solutions in flow estimation.

• In addition, it had been observed that the flow velocities measured at certain points along the channel axis have values close to the experimental data. Separations in the streamlines were also observed in the numerical solution at the point where the flow started to accelerate after reaching the critical depth.

• When the static pressure values affecting the channel bottom were examined, maximum values were obtained on the upstream aspect for both flow rates. In addition, negative pressure values were obtained in the region where the flow reached the critical depth and left the weir. This causes the risk of cavitation. For this reason, it may be recommended to cover the part where the negative pressure zone occurs with a more durable material.

In addition to all these, numerical solutions provide more precise solutions with new software developed every day. Its importance is gradually increasing. Different turbulence models, using this new design model, more sensitive results can be achieved. For this purpose, the effects of this type of broad-crested weir structure on the flow behavior can be seen in the numerical environment before being used in area applications. Especially durable materials can be preferred against the risk of wear on the weir surface. Appropriate design changes and measures can be taken accordingly. This broad-crested weir design can enable more efficient flow utilization in irrigation channels and environmental projects.

Acknowledgement

The author would like to thank the Inonu University Department of Civil Engineering for providing the use of the laboratory for the experiments and Dr. Fatih Kantarcı for helping.

REFERENCES

[1] Soydan Oksal NG, Akoz MS, Simsek O. Numerical modelling of trapezoidal weir flow with RANS, LES and DES models. Sādhanā. 2020;45(1):91.
[2] Felder S, Islam N. Hydraulic performance of an embankment weir with rough crest. J Hydraul Eng. 2017;143(3):4016086.
[3] Özlük A. Trapez Geniş Başlıklı Savaklara Ait Debi Katsayısının Yapay Zeka Yöntemleri İle Belirlenmesi. 2022.
[4] Hager WH, Schwalt M. Broad-crested weir. J Irrig Drain Eng. 1994;120(1):13–26.
[5] Tracy HJ. Discharge characteristics of broad-crested weirs. Vol. 397. US Department of the Interior, Geological Survey; 1957.
[6] Isaacs LT. Effects of laminar boundary layer on a model broad-crested weir. 1981;
[7] Faltas MS, Hanna SN, Abd-el-Malek MB. Linearised solution of a free-surface flow over a trapezoidal obstacle. Acta Mech. 1989;78:219–33.
[8] Clemmens AJ, Replogle JA, Reinink Y. Field predictability of flume and weir operating conditions. J Hydraul Eng. 1990;116(1):102–18.
[9] Sargison JE, Percy A. Hydraulics of broad-crested weirs with varying side slopes. J Irrig Drain Eng. 2009;135(1):115–8.
[10] Azimi AH, Rajaratnam N, Zhu DZ. Discharge characteristics of weirs of finite crest length with upstream and downstream ramps. J Irrig Drain Eng. 2013;139(1):75–83.
[11] Madadi MR, Dalir AH, Farsadizadeh D. Control of undular weir flow by changing of weir geometry. Flow Meas Instrum. 2013;34:160–7.
[12] Şimşek O, İşlek H, Aköz MS. Ağ Elemanı Özelliklerinin Sayısal Model Sonuçları Üzerine Etkisinin Belirlenmesi. Çukurova Üniversitesi Mühendislik-Mimarlık Fakültesi Derg. 2020;35(1):195–210.
[13] Sarker MA, Rhodes DG. Calculation of free-surface profile over a rectangular broad-crested weir. Flow Meas Instrum. 2004;15(4):215–9.
[14] Bal H. Geniş başlıklı savak içeren açık kanal akımının sayısal modellenmesi. Çukurova Üniversitesi, Adana, Türkiye. 2011;
[15] Felder S, Chanson H. Free-surface profiles, velocity and pressure distributions on a broad-crested weir: A physical study. J Irrig Drain Eng. 2012;138(12):1068–74.
[16] Soydan NG, Aköz MS, Şimşek O, Gümüş V. Trapez Kesitli Geniş Başlıklı Savak Akımının ke Tabanlı Türbülans Modelleri ile Sayısal Modellenmesi. Çukurova Üniversitesi Mühendislik-Mimarlık Fakültesi Derg. 2012;27(2):47–58.
[17] İlkentapar M, Öner AA. Geniş Başlıklı Savak Etrafındaki Akımın İncelenmesi. Niğde Ömer Halisdemir Üniversitesi Mühendislik Bilim Derg. 2017;6(2):615–26.
[18] YILDIZ MC, Yarar A. Geniş Başlıklı Savaklardaki Savak Yüklerinin Deneysel Ve Sayısal Olarak Modellenmesi. Konya J Eng Sci. 2020;8(1):164–74.

[19] Subramanya K. Flow in open channels. Tata McGraw-Hill; 2009.
[20] Raupach MR, Shaw RH. Averaging procedures for flow within vegetation canopies. Boundary-layer Meteorol. 1982;22(1):79–90.
[21] Guide AFT. ANSYS FLUENT Theory Guide. Release 18.2, 15317 (November). 2013;
[22] Hirt CW, Nichols BD. Volume of fluid (VOF) method for the dynamics of free boundaries. J Comput Phys. 1981;39(1):201–25.